

Spectroscopic trace gas analysis using semiconductor diode lasers

Peter Werle

Fraunhofer Institut für Atmosphärische Umweltforschung, Kreuzeckbahnstr. 19, D-82467 Garmisch-Partenkirchen, Germany

Accepted 23 October 1995

Abstract

Sensitivity, specificity, high time resolution, cost effective simultaneous measurements of several species and operational systems are the main requirements for in situ trace gas analysis in atmospheric research and process monitoring applications. Tunable diode laser absorption spectroscopy is increasingly being used to measure atmospheric trace gas concentrations down to low ppb-levels and the technique fulfills the requirements for trace gas analysis in the atmosphere for most of the smaller molecules with resolved absorption spectra. Semiconductor lead-salt diode-lasers give access to the mid infrared spectral region, where the most important atmospheric constituents have strong rotational vibrational absorption bands. The application of high frequency modulation (FM) schemes further improves sensitivity and detection speed of modern instrumentation. In this paper the FM technique will be reviewed with emphasis to the work, which has been done in our laboratory and findings from recent investigations, as well as novel approaches will be discussed. Some applications related to quality control and ISO calibration in addition to measurement challenges for fast and high sensitivity applications will be addressed.

Keywords: Diode laser; High resolution spectroscopy; Trace gas analysis

1. Introduction

Trace gas analysis at sub-ppb levels imposes high demands on analytic instrumentation. Since the development of lasers with high spectral brightness and tunability over broad wavelength ranges, laser based schemes are of growing interest. They are mostly based on absorption measurements. Since the absorption spectrum is characteristic for each molecule, spectroscopic methods allow highly specific detection of many substances. It is obvious that the mid infrared from 3 to 20 μm , the so-called “fingerprint re-

gion”, with strong rotational–vibrational absorption bands is the preferable wavelength range. Fast, accurate, rugged and operational instruments are needed for atmospheric research [1–6], environmental and process monitoring [7,8], medical diagnostics [9,10], plasma analysis [11] and many other applications [12–14].

Tunable diode laser absorption spectroscopy (TDLAS) usually applies multipass absorption cells to achieve high sensitivity. To alleviate problems by absorption line overlap, these absorption cells are usually operated at low pressure, where the linewidth is Doppler limited [15]. In most

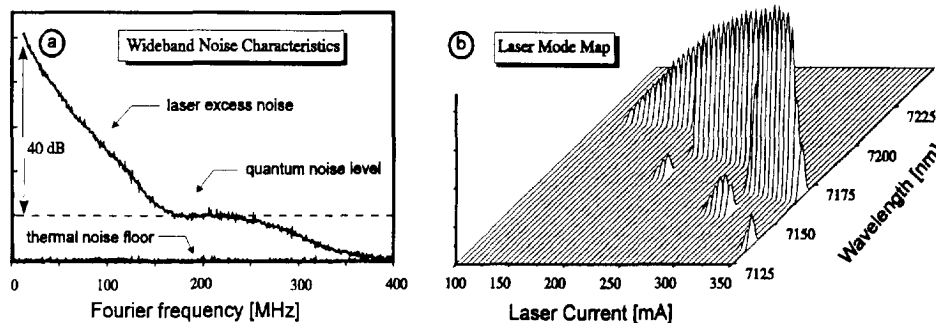


Fig. 1. (a) Wideband noise characteristics of a lead-salt diode-laser showing $1/f$ -type excess noise contributions up to 150 MHz. A signal-to-noise ratio improvement of about 40 dB can be expected when applying modulation frequencies in the quantum limited regime instead of low frequency modulation. (b) Laser excess noise contribution can be attributed to the presence of spurious side modes as indicated in the mode map near 200 and 300 mA.

sensitive instruments the diode laser is repetitively tuned over an absorption line of a target molecule and the absorption spectra are averaged over a specified time interval. Additional modulation techniques are used to reduce the $1/f$ -laser noise. With derivative spectroscopy using lock-in-detection at kHz modulation frequencies, typically, detection limits below 1 ppbv (1 ppbv = 10^{-9} volume mixing ratio) were achieved for many smaller molecules in the air with spectra averaging times of a few minutes [1–5]. Although these detection limits are sufficient for many applications, still better detection limits are required by modern atmospheric research [16].

Substantial improvements of TDLAS detection speed and detection limits were obtained by introducing the high frequency modulation (FM) technique [17–24]. However, to achieve the sensitivity improvement using the FM technique and to build instruments for routine high sensitivity measurements and even sensitive field applications, many practical problems still have to be solved [25,26]. In this paper, the principles of the FM-technique will be summarized and some limitations of the current instrumentation will be discussed.

2. FM-spectroscopy

High frequency modulation (FM) applied to tunable diode laser absorption spectroscopy has

the potential to satisfy most of the requirements for sensitivity, specificity, detection speed and applicability for many smaller molecules [17–24]. The FM technique, which was invented in 1979 by Bjorklund [17], determines the absorption or dispersion of a narrow spectral feature by detecting the heterodyne beat signal that appears when the FM optical spectrum of the probe wave is distorted by the spectral feature of interest. A modified two-tone modulation scheme has been introduced by Cooper and Gallagher [18] in 1984. A potential sensitivity improvement of up to two orders of magnitude in comparison to conventional derivative (2f) spectroscopy can be derived from wideband noise characteristics of lead-salt diode-lasers [26–30] for both FM-techniques. This sensitivity improvement can be achieved by increasing the modulation frequency from the $1/f$ -noise dominated region (10 kHz) into a shot noise limited domain of beyond 100 MHz [28]. A typical spectrum from a wideband noise measurement of a lead-salt diode-laser is shown in Fig. 1, where $1/f$ -type noise contribution can be identified up to frequencies between 100 and 200 MHz. The laser excess noise contributions can be attributed to the presence of spurious side modes shown in the laser mode map of Fig. 1 [26]. A signal-to-noise ratio improvement of about two orders of magnitude (40 dB) can be expected, when moving in detection frequency space to a quantum limited regime. Since the detection limit in FM-spectroscopy is then proportional to the square root

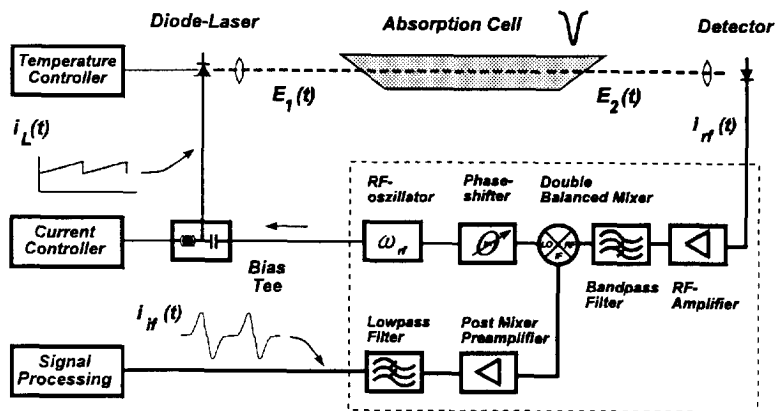


Fig. 2. Principle setup of a FM-spectrometer. To optimize the optical absorption pathlength mostly White or Herriott cells are used. The laser is repetitively tuned over an absorption line and after a phase sensitive detection the signal is further analyzed in a signal processing unit.

of the laser power on the detector, the laser output power should be as high as possible. This requirement is further stressed by the use of long absorption paths using multipass cells which strongly attenuate the incoming radiation [31]. The theoretical square root dependence of the detection limit on detector incoming power is only valid under quantum limited conditions, i.e. shot noise has to be the dominating noise source in the system. While the shot noise level depends on the incident photon flux, the thermal noise is independent of the laser power. Therefore, the laser power available after passing through the absorption cell should be high enough to generate a shot noise current, which is well above the thermal noise level.

The basic setup of a FM-spectrometer is shown in Fig. 2, where a rf-current (typically 100 MHz) is superimposed to a current ramp (typically kHz) and a DC current offset via a bias-tee to decouple the different current sources. The diode-laser is tuned by this injection current $i_L(t)$ and the electromagnetic field $E_1(t)$ of the laser interacts resonant with the rotational–vibrational absorptions of the molecules in the absorption cell. The interaction can be described by a complex transmission function $T(\omega)$ which accounts for absorption and dispersion. The electrical field after the probe $E_2(t)$ induces a detector current $i_{rf}(t)$, which is fed into the rf input of a double balanced mixer for

phase sensitive detection at the modulation frequency ω_{rf} . The time dependent demodulated signal $i_{IF}(t)$ at the IF port of the mixer is proportional to the concentration of the trace components in the absorption cell. The number of emitted photons depends upon the electron density in the conduction band and, therefore, from the injection current in the pn-junction of the diode laser. The higher the current, the higher the number of photons available and, therefore, the amplitude of the electromagnetic field depends on the photon density, i.e. changes in the laser current $i_L(t)$ will lead to an amplitude modulation of the laser light. The index of refraction in the pn-junction depends upon the carrier density as well. Due to this fact there is always a coupling between amplitude and frequency modulation for the electric field [32]. The formalism described here refers to the so-called single tone FM-technique [21]. In this case we can write for the complex phase modulated electrical field of the laser $E_1(t)$ with residual amplitude modulation

$$E_1(t) = E_0[1 + M \sin(\omega_{rf}t + \Psi)] \\ \times \exp\{i(\Omega t + \beta \sin(\omega_{rf}t))\}$$

where ω_{rf} is the modulation frequency, Ω is the laser frequency, β is the FM- and M the AM-index, and Ψ is the FM–AM-phaseshift or

$$E_1(t) = E_0 e^{i\Omega t} [1 + M \sin(\omega_{rf}t + \Psi)] \sum_{n=-\infty}^{+\infty} J_n(\beta) \\ \times e^{i n \omega_{rf}t} = E_0 \sum_{n=-\infty}^{+\infty} r_n(\beta, M, \Psi) \\ \times e^{i(\Omega + n \times \omega_{rf})t} \\ r_n(\beta, M, \Psi) = J_n(\beta) \\ + \frac{M}{2i} [J_{n-1}(\beta) e^{+i\Psi} - J_{n+1}(\beta) e^{-i\Psi}]$$

Pure amplitude modulation ($\beta = 0$) with $J_0(\beta = 0) = 1$ and $J_n(\beta = 0) = 0$ for $n = \pm 1, \pm 2, \pm 3, \dots$ shows three frequency components in the laser beam at Ω and $\Omega \pm \omega_{rf}$. Pure frequency modulation ($M = 0$) leads to sideband coefficients $r_n = J_n(\beta)$ and a 180° phase shift for upper and lower sidebands with odd n . In the general case the intensities of upper and lower sidebands with equal order n differ in magnitude due to the superposition of AM and FM signals. The complex electrical field after the probe is $E_2(t) = E_1(t)T(\omega)$, where $T(\omega) = \exp\{-\delta(\omega) - i\phi(\omega)\}$ is the complex transmission function with absorption $\delta(\omega)$ and dispersion $\phi(\omega)$ of the sample. $T(\omega)$ interacts with the individual frequency components ω_n and we obtain

$$E_2(t) = E_0 \sum_{n=-\infty}^{+\infty} r_n(\beta, M, \Psi) e^{i(\Omega + n \times \omega_{rf})t} e^{-\delta_n - i\phi_n}$$

with $\delta_n \equiv \delta(\omega_n)$, $\phi_n \equiv \phi(\omega_n)$, $\omega_n = \Omega + n \cdot \omega_{rf}$. Using $t = (\tilde{\nu}' - \tilde{\nu}_0/\gamma_D)(\sqrt{\ln 2})$, $x = (\tilde{\nu}' - \tilde{\nu}_0/\gamma_D) \times (\sqrt{\ln 2})$ and $y = (\gamma_L/\gamma_D)(\sqrt{\ln 2})$ we obtain for a Voigt profile [15]

$$\delta_\nu(\omega) = \frac{l}{2} \frac{S}{\gamma_D} \sqrt{\frac{\ln 2}{\pi}} c V(x, y)$$

$$V(x, y) = \frac{y}{\pi} \int_{-\infty}^{+\infty} \frac{\exp\{-t^2\}}{y^2 + (x-t)^2} dt$$

$$\phi_\nu(\omega) = \frac{l}{2} \frac{S}{\gamma_D} \sqrt{\frac{\ln 2}{\pi}} c L(x, y)$$

$$L(x, y) = \frac{1}{\pi} \int_{-\infty}^{+\infty} \frac{(x-t) \exp\{-t^2\}}{y^2 + (x-t)^2} dt$$

where γ_D is the Doppler width and γ_L is the

pressure broadened Lorentzian linewidth. S is the line strength, ν_0 the frequency at line center and l the absorption pathlength. The absorption at line center $\delta_{\nu, \text{peak}}(x = 0)$ is

$$\delta_{\nu, \text{peak}} = \frac{l}{2} \delta(\nu_0) c = \frac{l}{2} \frac{S}{\gamma_D} \sqrt{\frac{\ln 2}{\pi}} V(0, y) c$$

The laser beam induces a photo current at the modulation frequency ω_{rf} at the square law detector element, thus

$$i_{rf}(t) = \text{const} |E_2(t)|^2 = \text{const} |E_0|^2 \\ \times \sum_{n, n' = -\infty}^{+\infty} r_n \bar{r}_{n'} e^{i(n-n')\omega_{rf}t} e^{-\delta_n - \delta_{n'}} e^{-i(\phi_n - \phi_{n'})}$$

If we account for the detector high frequency rolloff and apply a narrow band detection at the modulation frequency using a double balanced mixer, we can neglect the contributions proportional to $\exp(\pm im\omega_{rf}t)$ for $m = 2, 3, 4, \dots$. Therefore the indices n' are limited to $n' = n \pm 1$ and we obtain

$$i_{rf}(t) = i_0 \{Z e^{i\omega_{rf}t} + \bar{Z} e^{-i\omega_{rf}t}\} \\ Z = \sum_{n=-\infty}^{+\infty} r_{n+1} \bar{r}_n e^{-\delta_{n+1} - \delta_n} e^{-i(\phi_{n+1} - \phi_n)}$$

If we define $A = 2 \text{Re}(Z)$ and $D = -2\text{Im}(Z)$ we obtain for the rf-current i_{rf} , the local oscillator signal i_{LO} , and i_{IF} signal at the output of the mixer

$$i_{rf}(t) = i_0 \{A \cos(\omega_{rf}t) + D \sin(\omega_{rf}t)\}$$

$$i_{LO}(t) = i_{LO,0} \sin(\omega_{rf}t + \Theta)$$

$$i_{IF}(t) = \langle i_{rf}(t) i_{LO}(t) \rangle_\tau$$

where Θ is the phase shift. We obtain after low-pass filtering of sum frequency components at $(2\omega_{rf}t + \Theta)$ with a time constant τ as a detectable signal after the post mixer preamplifier

$$i_{IF} = \frac{1}{2} i_0 \{A(\beta, M, \Psi) \sin \Theta + D(\beta, M, \Psi) \cos \Theta\}$$

Depending on the detection phase Θ , selectively the absorption ($\Theta = \pi/2$) or dispersion ($\Theta = 0$) of a spectral feature can be measured. With the above definitions for A , D , and Z and using $r_{n+1} \bar{r}_n = R_n + iI_n$ we can write for the general case for arbitrary AM–FM phaseshifts Ψ

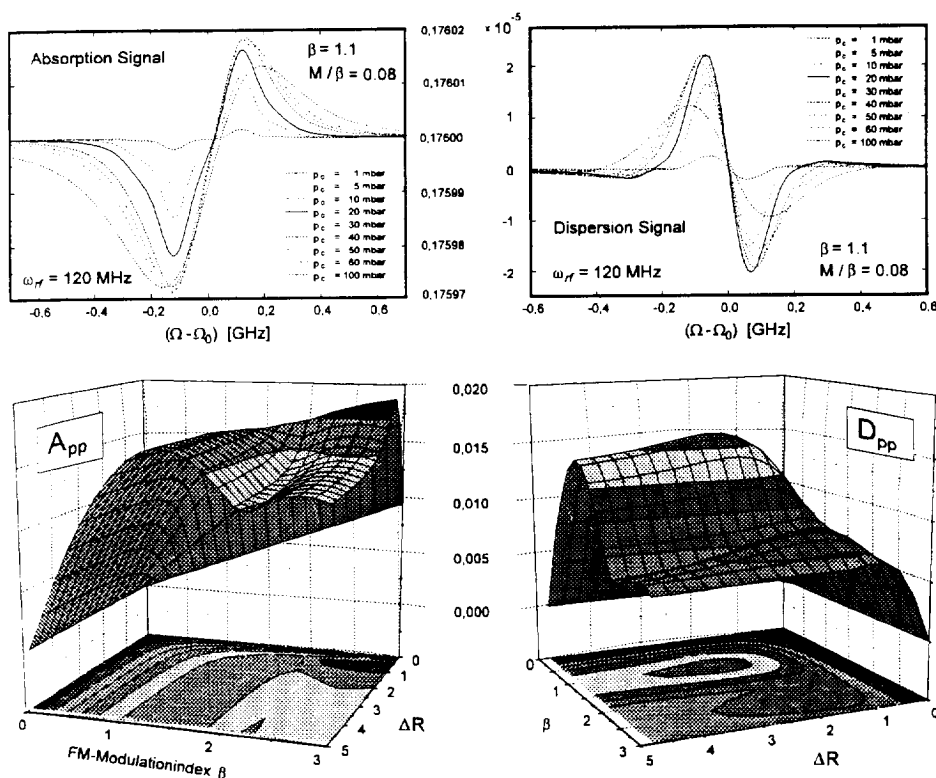


Fig. 3. Calculated absorption and dispersion signals in the absorption cell for pressures ranging from 1 to 100 mbar. Note the strong DC-offset for the absorption signal, while the dispersion signal has zero offset. The optimum dispersion signal is obtained at about 30 mbar pressure in the multipass cell. The calculated peak-to-peak FM-signals for absorption A_{pp} and dispersion signals D_{pp} are shown in the lower part of the figure as a function of the FM modulation index β and the ratio ΔR of the modulation frequency to the half width at half maximum (HWHM) of the absorption feature.

$$A = 2 \sum_{n=-\infty}^{+\infty} \{R_n \cos(\phi_{n+1} - \phi_n) + I_n \sin(\phi_{n+1} - \phi_n)\} e^{-\delta_{n+1} - \delta_n}$$

$$D = -2 \sum_{n=-\infty}^{+\infty} \{I_n \cos(\phi_{n+1} - \phi_n) - R_n \sin(\phi_{n+1} - \phi_n)\} e^{-\delta_{n+1} - \delta_n}$$

$$R_n = J_{n+1}J_n + \frac{M}{2} \{k_1 + k_2\} \sin \Psi + \left(\frac{M}{2}\right)^2 \{k_3 - k_4 \cos(2\Psi)\}$$

$$I_n = \frac{M}{2} \{-k_1 + k_2\} \cos \Psi + \left(\frac{M}{2}\right) k_5 \sin(2\Psi)$$

$$\left. \begin{aligned} k_1 &= (J_n)^2 + (J_{n+1})^2 \\ k_2 &= J_{n-1}J_{n+1} + J_nJ_{n+2} \\ k_3 &= J_nJ_{n-1} + J_{n+1}J_{n+2} \\ k_4 &= J_{n-1}J_{n+2} + J_nJ_{n+1} \\ k_5 &= J_{n-1}J_{n+2} - J_nJ_{n+1} \end{aligned} \right\} J_v = J_v(\beta)$$

Using the formulas derived above in a computer program, the line shapes for arbitrary FM-signals can be calculated. This is useful for line fitting procedures during spectral analysis, for the deconvolution of FM-spectra, estimation of unknown spectral parameters like AM-FM-phaseshift Ψ and for the prediction of system performance from system parameters. The latter point is important for system calibration under conditions

where calibration by gas mixtures is difficult. Problems arise, for example, during the measurement of free radicals, polar substances, etc., where due to lifetime, wall effects or sealed sample cells the standard calibration schemes, which base on a measurement sequence of calibration gas, zero air and sample air within the same multipass cell, do not work. There is experimental evidence that diode lasers have at frequencies around 100 MHz an AM–FM phaseshift of $\Psi = \pi/2$ [33]. From the asymmetry of the signals and from Fabry–Perot analysis of the laser sidebands the ratio M/β has been estimated to be below 0.1 in general [21]. A calculated plot of a typical absorption and dispersion signal is shown in Fig. 3 for pressures ranging from 1 to 100 mbar. The calculated peak-to-peak FM-signals for absorption A_{pp} and dispersion signals D_{pp} as a function of the FM-index β and the ratio $\Delta R = \omega_{rf}/\text{HWHM}$ for an AM/FM ratio $M/\beta = 8\%$, $\delta_{\text{peak}} = 0.01$ and $\Psi = \pi/2$ are shown in the 3D-plot in the lower part of Fig. 3. It can be seen that a broad maximum for the absorption and dispersion signal can be found around values for $\beta = 1.1$. The modulation frequency should be chosen at least 1.6 times the half width at half maximum (HWHM) of the spectral feature under investigation.

For a better understanding of the signal generation it is interesting to investigate the special case of $\Psi = \pi/2$, the limit of low modulation $\beta \ll 1$, $M \ll 1$ and additionally the limit of low absorption $\delta_n \ll 1$ and dispersion $\phi_n \ll 1$. In the special case we obtain $i_{FM} = A \sin \Theta + D \cos \Theta$ with $A = 2\beta \Delta \delta$ and $D = 2\beta \Delta \phi$ where the dispersion and absorption component is given as $\Delta \phi = (2\phi_0 - \phi_{-1} - \phi_{+1})$ and $\Delta \delta = (\delta_{+1} - \delta_{-1})$ in agreement with the formulas originally presented by Bjorklund [17].

3. Detection limit and system stability

The signal-to-noise-ratio (SNR) is a convenient way to describe the “cleanliness” of a given signal level. It is the signal voltage (or power) divided by the RMS-noise voltage (power). A spectrum obtained with a SNR of 100 or more is a very clean pattern, with negligible noise. An SNR of 10 is a

little fuzzy, but the pattern is still very clear. A ratio of 3 is bad and at 1 the signal is nearly lost. If the noise in the detection system is the limiting factor for ultimate sensitivity, the detection limit of a spectrometer can be derived from the signal-to-noise ratio referring to the output of a preamplifier with a noise figure F :

$$\text{SNR}_P = \frac{1}{F} \text{SNR}_P^{\text{Det}} = \frac{1}{F} \frac{\langle i_S^2 \rangle}{\langle i_N^2 \rangle}$$

The three main noise contributions which have to be considered are the thermal noise of the detector preamplifier combination, i_{th}^2 , the quantum (shot) noise, i_{sn}^2 , and a $1/f$ -type laser excess noise, $i_{1/f}^2$. While thermal noise and quantum noise have in general a frequency independent spectrum (white noise), the $1/f$ -noise contribution has a more or less pronounced frequency dependence (pink noise). To achieve quantum limited operation the modulation frequency has to move in detection frequency space into a domain, where $1/f$ -noise contributions can be neglected. If sufficient power is available, the power independent thermal noise can be neglected as well and shot noise remains to be the dominating noise contribution. If this can be achieved the SNR is proportional to the square root of the laser power impinging upon the detector. As can be seen from Fig. 1, there are regions at modulation frequencies above 100 MHz where a $1/f$ -noise contribution can be neglected. If we move in detection frequency range into such a potential quantum limited regime, we can approximate the total noise as the sum of shot noise and thermal noise

$$\begin{aligned} \langle i_N^2 \rangle &\cong \langle i_{sn}^2 \rangle + \langle i_{th}^2 \rangle \\ &\cong 2e \langle i_{dc} \rangle \Delta f + 4k_B(T/R)_{\text{eff}} \Delta f \end{aligned}$$

$$\langle i_{dc} \rangle = i_0 + i_D = e\eta \lambda P_D / hc + i_D$$

P_D is the power of the laser light at the detector element, i_D is the detector dark current, Δf the system bandwidth and T/R the temperature-resistance-ratio of the detector preamplifier combination. The measured signal is proportional to the laser power incident upon the detector. As the dispersion signal has no DC offset, we investigate the signal current at the rf-modulation frequency, which has been derived as $i_s = i_0 D \sin(\omega_{rf} t)$. The

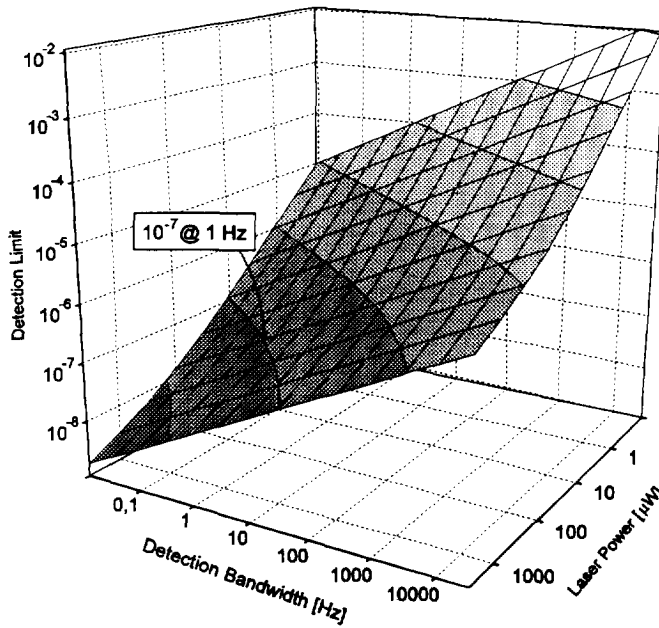


Fig. 4. Calculated minimum detectable absorbance as a function of detection bandwidth Δf and laser power P_D incident upon the detector element.

power associated with this signal is

$$\langle i_s^2 \rangle = \frac{1}{2} i_0^2 D^2$$

and the resulting SNR is

$$\begin{aligned} \text{SNR}_p &= \frac{1}{F} \frac{\langle i_s^2 \rangle}{\langle i_N^2 \rangle} \\ &= \frac{1}{2F} \frac{i_0^2}{2e(i_0 + i_D) + 4k_B(T/R)_{\text{eff}}} \frac{1}{\Delta f} D^2 \end{aligned}$$

The detection limit in terms of the minimum detectable optical density OD_{min} for a $\text{SNR}_p = 1$ at $\Delta f = 1$ Hz is

$$\begin{aligned} \text{OD}_{\text{min}} = 2\delta_{\text{peak}}^{\text{min}} &= 2 \frac{D_{pp}(\text{SNR} = 1)}{\kappa_D} = \frac{2hc\sqrt{2F}}{e\eta\lambda\kappa_D P_D} \\ &\times \sqrt{\frac{2e^2\eta\lambda}{hc} P_D + \{2ei_D + 4k_B(T/R)_{\text{eff}}\}} \end{aligned}$$

Using the equation derived above we can calculate an estimate for the detection limit for typical experimental parameters. The ratio κ_D can be derived from the 3D plots in Fig. 3 to be about 1.6. The laser power P_D at the detector with a

specified quantum efficiency $\eta_{\text{cw}} = 50\%$ was about $100 \mu\text{W}$. For a given set of experimental conditions ($\lambda, \eta, i_D, \beta, M$) the noise figure F has to be minimized, while the impedance match between the detector and the preamplifier has to be optimized as well. Due to limited laser power and reflection losses in optical multipass systems measurements often are not quantum limited, as the shot noise from the light independent contribution of the dark current and the thermal noise from the detector/preamplifier combination were dominating. Typically, the quantum efficiency is specified under cw illumination. For a system analysis it is necessary to consider the quantum efficiency at the modulation frequency, which can be significantly below its cw value. If we assume $\eta_{\text{eff}} \approx 0.4$ we obtain for the minimum detectable optical density $\text{OD}_{\text{min}} \approx 4.4 \times 10^{-7}$ at 1 Hz. Fig. 4 illustrates the dependence of the detection limit for a given set of experimental parameters:

$$\text{OD}_{\text{min}} \propto \sqrt{F} \sqrt{\Delta f} \sqrt{\frac{1 + (P_0/P_D)}{P_D}}$$

There are actually two possible directions towards

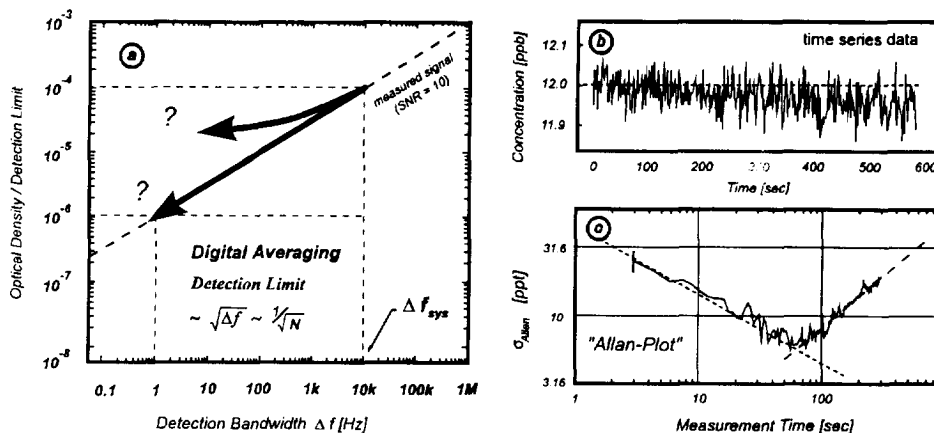


Fig. 5. (a) System stability: How long can we average spectra? (b) Time series data from a 12 ppb NO_2 calibration gas mixture and (c) the corresponding "Allan-plot" as a function of the integration time. The minimum indicates that most sensitive measurements can be achieved with about 60 s integration time. As no drift should occur between background and sample measurement, the maximum available averaging time is 25 s, yielding a detection limit of about 10 ppt.

lower detection limits: increasing the laser power on the detector and bandwidth reduction. For a laser power $P_D \gg P_0$ the detection limit is proportional to $P_D^{-1/2}$, for $P_D \ll P_0$ it is proportional to P_D^{-1} . The power level P_0 , where shot noise equals the dark current and thermal noise is about several hundred μW , while the typical power output from commercially available lasers varies between 10 and 1000 μW . The second direction for further improvement of the sensitivity is digital signal averaging, which is equivalent to an electronic bandwidth reduction. Therefore, some problems associated with signal averaging will be discussed next.

In addition to laser performance, a second critical factor influencing the high sensitivity measurements is the system stability, especially at low optical densities below 10^{-5} . At these sensitivities interference fringes due to unwanted étalons are becoming the factor limiting further improvement of the detection limits [25]. To achieve the aforementioned detectable optical density, several techniques to reduce the magnitude of these fringes had to be applied, such as a dithered Brewster angle plate or mirror [34], low frequency jitter of the laser current or low pass filtering. A substantial further improvement of the TDLAS sensitivity by these and similar techniques or their combination is hard to achieve. In principle, the problem of

fringe limitation can be solved by subtraction of a background spectrum from the measurement spectrum. Trace gas measurements near to the detection limit are, therefore, usually performed by measuring alternatively the spectrum of the ambient air and the spectrum of zero air, i.e. air devoid of the target substance. This procedure is based on the inherent assumption that within the time interval needed for the acquisition of both the measurement and the background spectra, the fringes do not move. If this assumption is fulfilled, the subtraction of the background spectrum from the measurement spectrum would provide the absorption spectrum of the target species which, to a first approximation, is only subject to random noise. Further averaging of these corrected spectra should then improve the detection limit according to a square root relationship. This behaviour is illustrated in Fig. 5a. If we assume a TDLAS spectrometer capable of detecting an optical density of 10^{-4} at the system detection bandwidth Δf_{sys} with a signal-to-noise ratio (SNR) of 10; this corresponds to a detection limit (with SNR = 1) of 10^{-5} at 10 kHz. By averaging 10^4 spectra, the effective bandwidth of the instrument will be reduced to 1 Hz and this reduction should result in a detection limit of 10^{-7} at SNR = 1. This has been tried but the achieved improvement was always substantially smaller than that one

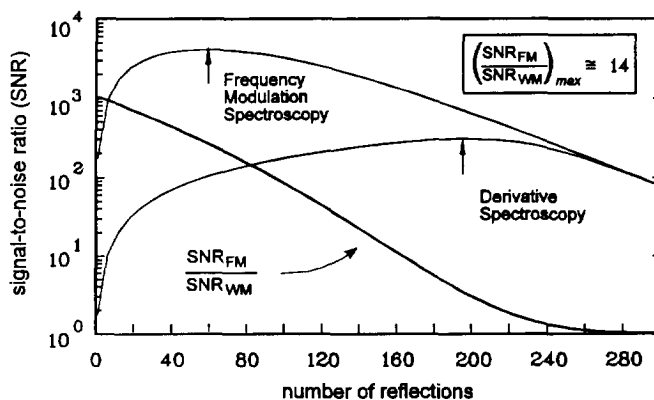


Fig. 6. Signal-to-noise ratio analysis in optical multipass cells: owing to the attenuation of the laser beam in the FM case the SNR has a mixture at a lower number of reflections than in the case of derivative spectroscopy.

expected on the basis of the square root relationship. The observed deviations are most probably caused by the violation of the above assumption of stationarity and, consequently, the stability of the TDLAS instrument has to be investigated.

In principle, the signal from a perfectly stable system could be averaged infinitely. Infinite averaging should lead to extremely sensitive measurements, if limitations of the dynamic range of the system are neglected. Unfortunately, real systems are not stable forever and the question is, how long can signals be averaged to achieve an optimum sensitivity with a given spectrometer? It is obvious that every real world spectrometer will have an optimum averaging time given by the drifts in the system, such as temperature drifts, moving fringes, background changes, etc. The instrument stability as a figure of merit can be described using the Allan variance [25].

$$\langle \sigma_A^2(\tau) \rangle_t = \frac{1}{2m} \sum_{s=1}^m (A_{s+1}(\tau) - A_s(\tau))^2$$

The Allan variance [35–37] is the time average of the sample variance of two adjacent averages A_{s+1} and A_s of time series data, taken during an integration interval τ . Noise contributions, which are encountered in most systems are frequency independent, white noise and frequency dependent $1/f$ - and $1/f^2$ -noise. The last is noise at very low frequencies, which can be considered as drift. The detection limit expressed in terms of the Allan variance improves with increasing integra-

tion time. For white noise dominated processes the Allan variance is equivalent to the conventional variance and can be used to predict the detection limit of a given system as a function of the integration time. Allan variance of time series data (Fig. 5b) plotted as a function of the integration time leads to the “Allan plot” [25,37], such as shown in Fig. 5c. The minimum of the Allan variance corresponds to the optimum integration time, typically on the order of 40–100 s. This has been confirmed by many other researchers [38,39]. The optimum integration time is a characteristic property for a given instrument, as it reflects the overall system stability and performance.

4. Current limitations in FM-spectroscopy with optical multipass cells

The optical densities that have to be detected in trace gas analysis applications are usually small ($< 10^{-5}$), and to achieve sensitivity adequate for environmental monitoring, absorption spectrometers require long optical paths. In instruments with a limited size, long absorption pathlengths up to several hundreds of meters have usually been provided by multi-reflection optical systems, of which the most well known are the systems invented by White and by Herriott [40–42]. In all these systems the sensitivity gained by lengthening the absorption path is offset by the increasing attenuation of the radiation power throughput,

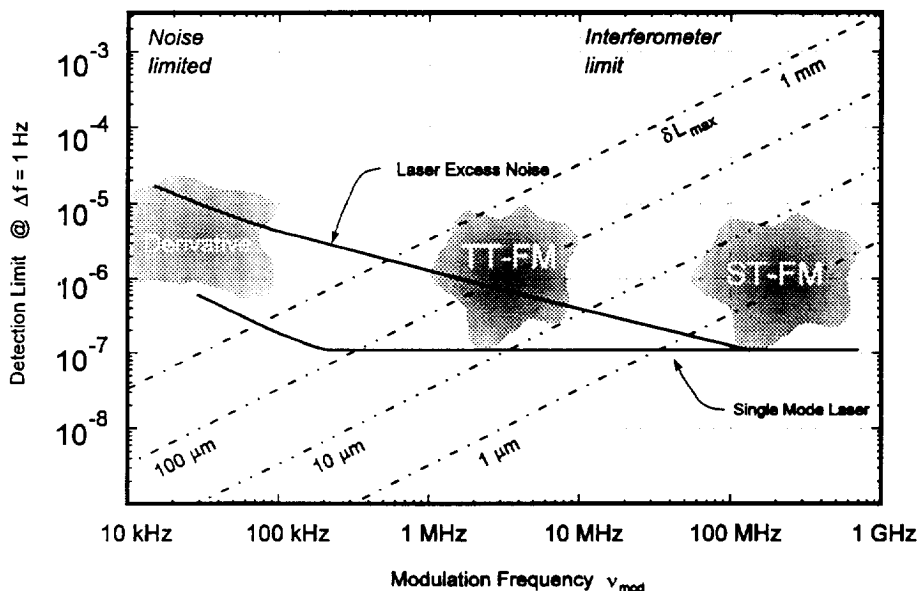


Fig. 7. Detection limit in terms of optical density as a function of the laser modulation frequency ν_{mod} for different assumptions on mechanical system stability δL and for a laser with and without excess noise at high frequencies.

due to the imperfect reflectivity of the mirrors. Consequently, to achieve the highest SNR each absorption spectrometer has to be operated with an optimal number of reflections in multi pass systems. In high resolution absorption spectrometers with conventional light sources, the signal-to-noise ratio (SNR) is usually limited by the thermal noise level of the detector–preamplifier combination, which is independent of the light source power. However, the noise in many laser absorption spectrometers is dominated by the excess or shot noise, which depends on the transmitted laser power, and, therefore, depends on the number of reflections in a multipass cell [31]. The signal-to-noise ratio in optical multipass cells used for monitoring trace gas concentrations is shown in Fig. 6 for high frequency modulation (FM) as well as conventional derivative (WM) laser absorption spectrometers. At conditions usually encountered in tunable diode laser spectrometers the optimal number of passes for the FM spectrometers has been found to be much smaller than the optimal number of passes for the WM spectrometers. This finding implies that if both techniques are operated with an optimal number of passes, the introduction of FM techniques can improve

the SNR in spectrometers using optical multipass cells by only about an order of magnitude (Fig. 6). Although still highly desirable, this is substantially lower than the two orders of magnitude potential improvement derived solely from the noise analysis, without considering the use of multipass cells [28]. The smaller number of passes required for optimal SNR in FM spectrometers has other practical consequences. Cells with a smaller number of passes are cheaper to construct and to adjust. As they can be designed with smaller volume, faster measurements can be made. This property is important because only in small volume cells can high speed FM measurements be performed. If, on the other hand, ultra-sensitive measurements require a long absorption pathlength, high reflectivity mirrors and high power lasers are a prerequisite to get the full potential of FM techniques.

As mentioned previously, the $1/f$ -type laser excess noise can be attributed at least in part to the presence of sometimes spurious side-modes [26]. Consequently with state-of-the-art lead-salt diode-lasers, high modulation frequencies are necessary to achieve near shot noise limited performance of the FM spectrometer. On the other hand a FM

spectrometer can be interpreted as a two-color interferometer [26,43] and, therefore, it is extremely sensitive to thermal drifts in the optical setup. With increasing modulation frequency, i.e. high separation of FM sidebands in the frequency domain, the sensitivity of the FM spectrometer towards fluctuations in the optical path increases. Therefore, low modulation frequencies should be used to achieve a high system stability during long integration times. This is illustrated in Fig. 7. If we assume the laser excess noise from Fig. 1, the system detection limits range from about 10^{-5} (at 10 kHz) down to 5×10^{-7} (at 10 MHz). If we further assume a mechanical system stability of 10 μm , we can see from Fig. 7 that the detection limit again becomes worse for higher modulation frequencies due to interferometric effects. Only with single mode lasers could these problems be avoided. Signal instabilities at low optical densities caused by interferometric effects might give an explanation for the fact, that the expected improvement in system performance after the application of high frequency modulation schemes to spectroscopic systems designed for conventional derivative spectroscopy has not yet been attained on a routine basis. The interferometric effect at high modulation frequencies is superimposed to the so called 'etalon-effect'. In most sensitive instruments the diode laser is repetitively tuned over a molecular absorption line and the spectra are averaged over a specified time interval. When the wavelength of the diode laser is tuned over an absorption line, a periodic fringe structure can be superimposed to the desired signal from the absorption of the target gas. If this fringe structure is generated between the reflecting mirrors in the multipass absorption cell, mechanical drifts cause a change of the fringe structure. These time varying structures usually limit sensitivity if they cannot be suppressed sufficiently [34]. But even if the losses which are responsible for the 'etalon-effect' could be eliminated, e.g. by an optical isolator, the above mentioned 'interferometer-effect' remains and for sensitive measurements, say at optical densities below 10^{-6} , short term changes in the optical setup of only a few μm can influence system performance significantly. Therefore, interferometric stability is required for the opto-

mechanical setup of a sensitive FM spectrometer, which can be very expensive. An alternative approach is the time consuming selection of single mode lead-salt diode-lasers with several mW power, with low $1/f$ -noise, but unfortunately such lasers are not available for many desired wavelengths. With state-of-the-art FM-TDLAS spectrometers, system optimization is often a trade-off between limitations due to laser excess noise and limitations caused by interferometric effects. Therefore, further development and commercial availability of high power, single mode lead-salt diode-lasers with distributed feedback (DFB) structures would really help to improve spectrometer performance in the IR for routine applications.

The interferometric effect has other important consequences. In a recent publication [44] we discussed the influence of refractive index fluctuations caused by the turbulent flow of the air sample through the multipass cell. Fig. 8 shows a plot of the detection limit in terms of phase jitter plotted vs. the pressure fluctuation in the absorption cell. Superimposed to the "quantum limit" is the phase jitter, caused by the refractive index fluctuations, which again are due to pressure changes in the cell. For modulation frequencies of 100 MHz the expected relationship between phase and pressure fluctuations for a pathlength of 100 m is plotted. Due to turbulent refractive index fluctuations, we obtain a limit of about 7×10^{-7} in terms of optical density for a modulation frequency of about 100 MHz. The data were derived from measurements like the 3D-plot in Fig. 8, where the Fourier spectra of pressure fluctuations in the multipass absorption cell up to 20 kHz are displayed for gas flows up to 10 l min^{-1} through the cell. The estimated detection limit from such measurements is significantly above the quantum limit, as indicated by the shaded area in Fig. 8.

One might get the impression, that the use of lower modulation frequency should improve the situation. But system operation at lower modulation frequencies, say 10 MHz or even lower, has to be investigated carefully, because one might run into limitations due to laser excess noise [26]. This is especially important for mid infrared spectrometers using lead-salt diode-lasers, where the

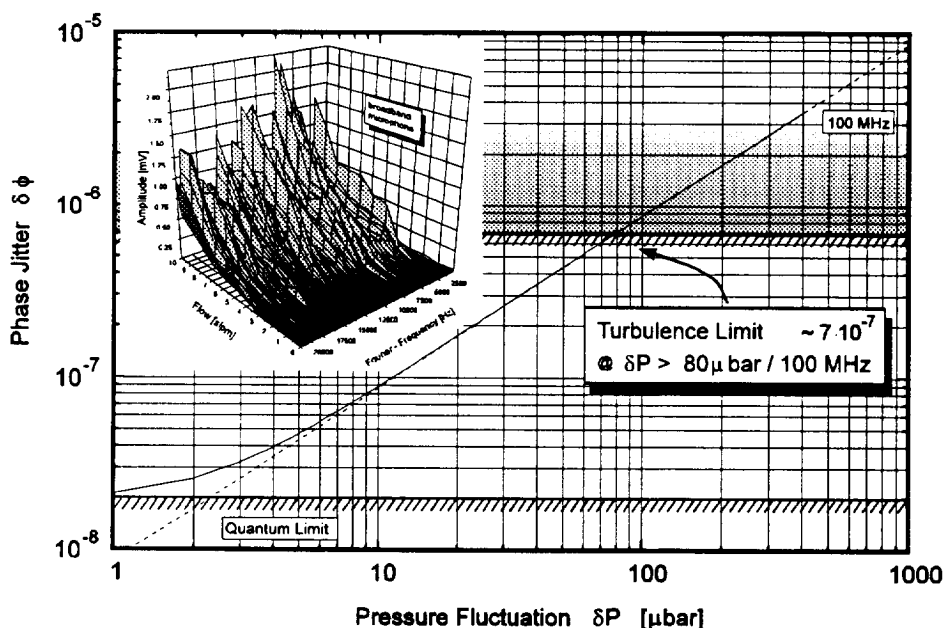


Fig. 8. Detection limit in terms of the phase jitter generated from pressure fluctuations in the optical multi pass cell. The 3D-plot illustrates that pressure fluctuations up to 20 kHz increase with increasing gas flow through the absorption cell.

presence of even spurious side modes substantially increases the laser excess noise, even at 10 MHz and, in order to obtain a quantum limited performance, these excess noise contributions have to be avoided. We have limited the discussion of refractive index fluctuations so far to FM-spectrometers, because they have the potential to reach the quantum limit, which has been demonstrated with short absorption cells [20,21]. However, turbulence effects might also be important for conventional, derivative or direct absorption spectrometers and we are not aware of any investigation on the effect of turbulence in multipass cells on beam wander, angle-of-arrival fluctuations, intensity fluctuations and beam broadening. Such effects should occur, when a laser beam propagates through a large number of refractive index inhomogeneities and the cumulative effect can be very significant. Modern multipass cell designs [42] already utilize an improved gas flow, in order to obtain a laminar flow for fast exchange times and, therefore, we expect such a Herriott-type cell to be superior for ultrasensitive measurements at low optical densities. At least,

there seems to be evidence for a significant contribution of turbulent refractive index fluctuations to the detection limit of state-of-the-art FM-spectrometers using atmospheric open paths [39] and optical multipass cells and we think this effect should be considered for systems, designed for near quantum limited applications.

5. Modern signal processing concepts

While many instrumental improvements in tunable diode laser absorption spectroscopy focus on optical stabilization schemes [45,46], much less effort has been put into post detection signal processing [47,48]. Spectroscopic signals vary in frequency due to fluctuations or transients in the laser current and they vary in amplitude due to changes in background radiation, laser intensity and time dependent fringe structures. Therefore, a signal processing concept for TDLAS must provide means for correcting frequency and amplitude fluctuations as well as having some ability to cope with changing background structures.

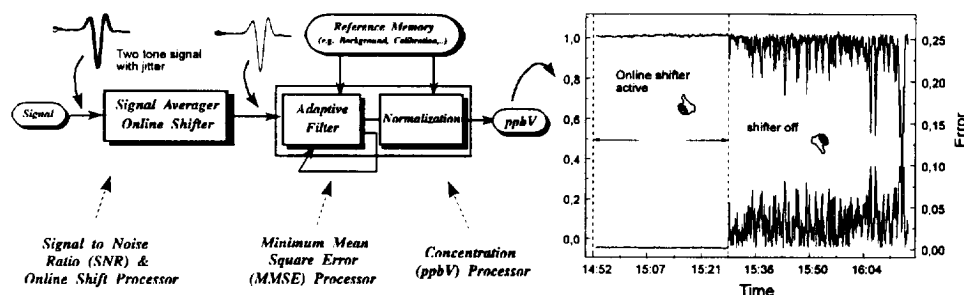


Fig. 9. Signal processing strategies for tunable diode laser spectroscopy: the application of an online shift procedure to remove jitter from FM spectra improves significantly the quality of concentration data, as can be seen from the associated errors.

Most critical is the impact of drifts of ambient spectra relative to the previously recorded calibration spectrum. These drift effects can lead to a significant underestimation of concentration values, i.e. a spectrometer might report extremely low concentration values and possible variations in calculated data can rather refer to drift effects than to changes in ambient trace gas concentrations. Fluctuations in the laser current due to noise and other interfering signals have a significant influence on the system performance, especially on the confidence range of the measurement [25] and, therefore, on the detection limit of the system. A useful approach is to correct such drifts and jitter online during the averaging process [48]. An example is shown in Fig. 9, where the effect of an online shift correction on a two-tone FM signal with jitter is demonstrated. If we record a calibration signal and then continue to sample the same signal as ambient, we expect the fit process to report a concentration (ratio of ambient to calibration signal) of unity, as it is shown in the time series plot of Fig. 9, when the shifter is active. As soon as the shifter process is turned off, significant deviations from the true value can be observed and the associated errors increase dramatically as well. Variations in the signal amplitude can be corrected by intensity normalization. A novel concept is based on the measurement of the average modulation signal amplitude instead of measuring detector currents or reference signals [48]. With high frequency modulation techniques, the rf-power level at the detector ideally reflects variations in laser power and system alignment changes due to slow drifts. While conventional intensity normalization schemes use a reference

channel or the detector bias current, this normalization is independent from changes in background radiation and a detailed investigation of signal stability using the Allan variance analysis indicated improved stability. Background changes can, at least in part, be attributed to time dependent fringe drifts and in many cases a slope or curvature has been observed. Varying slopes can also be obtained from pressure broadened atmospheric absorption lines (e.g. water vapour). Such a situation calls for the introduction of adaptivity. Multiple linear regression schemes and adaptive filters [47,48] use a minimum mean square error algorithm to determine an optimum set of coefficients for a filter. For each ambient spectrum a calculation of the filter coefficients is performed and, therefore, the filter is able to adapt to changing conditions, such as signal drift and changing background structures. Such a digital filter has the interesting feature that, in principle, besides ambient and calibration spectra no further information is needed. This technique might allow less frequent or even no background sampling and, therefore, is well suited for fast measurements.

Further progress in sensitivity of current diode laser spectrometers practically depends on improved lasers and increased system stability. As the FM technique originally has been referred to as a zero-baseline technique [17] this is no longer valid for trace gas measurements near the detection limit, because the background is changing with time. Therefore, it is important to measure as fast as possible alternating the sample and the background spectra, especially at low concentration levels. The switching time from ambient to background measurements is usually limited by

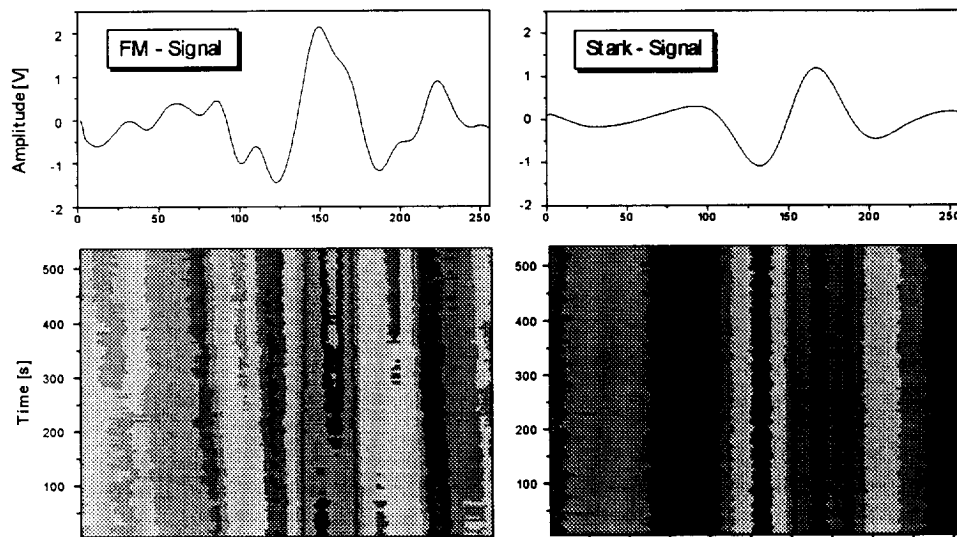


Fig. 10. Active stabilization of a FM-signal obtained by a FM-Stark double modulation technique: drift effects caused by moving fringe structures can be observed with conventional FM-spectroscopy, while after the application of an additional Stark-sample modulation a significantly higher stability has been obtained.

the exchange time of the gas, which is typically in the order of seconds. For sensitive and precise measurements this might be too long and, therefore, different approaches have to be tried. One approach is to increase the pumping speed using minimized multi-pass absorption cells. A 36 m Herriott cell with an exchange time as low as 50 ms ($1/e$) has been developed recently [42]. An alternative approach is the use of photochemical sample modulation [49]. In a similar way a combination of laser-FM and Stark-sample-modulation has been applied successfully to suppress background fluctuations and drifts [50]. An example of the application of such a double modulation is shown in Fig. 10, where spectra have been monitored for about 10 min for FM spectroscopy and for a combined FM–Stark double modulation technique. While the drift effects caused by moving fringe structures can be clearly identified in the FM signal, a significantly higher stability has been obtained in the double modulation case. Fortunately some molecules of major interest in atmospheric chemistry, such as formaldehyde and hydrogen peroxide, exhibit a strong electric dipole moment as indicated in Table 1, which shows a list of selected molecules of interest and the calcu-

lated detection limits under the assumption of a minimum detectable absorbance of 10^{-6} within 1 s integration time and an absorption path length of about 25 m at a pressure of 30 mbar using a multipass cell. The calculated detection limits scale linear with the minimum detectable absorbance and the absorption pathlength. However, for the calculations only 25 m absorption path in the multipass cell have been assumed as the power loss due to the multiple reflections on the mirrors overcompensates the sensitivity gain due to a longer absorption path [28]. The optimum pathlength for a given system can be estimated from system parameters (laser power, mirror reflectivity) and we found 25 m best suited for our experimental setup with a White cell. Higher sensitivities are expected at longer integration times for a stable system.

6. Applications to measurement challenges in atmospheric chemistry

Due to the sensitivity enhancements in modern instrumentation more and more systems are used in field applications for the detection of low con-

Table 1
 Calculated 1 σ -detection Limits DL for a minimum detectable absorbance of 10^{-6} at 30 mbar in 25 m multi path cell at 296 K, $S \equiv$ line strength, $\sigma_0 \equiv$ absorption cross section at line center, $\gamma_V \equiv$ Voigt-HWHM

Gas	μ /Debye	$\tilde{\nu}_0/\text{cm}^{-1}$	$\lambda/\mu\text{m}$	$S/10^{-20}/\text{cm mole}^{-1}$	$\gamma_V/10^{-3} \text{ cm}^{-1}$	MHz	$\sigma_0/10^{-18}/\text{cm}^2 \text{ mole}^{-1}$	$c_{\text{min}}^{\text{STP}}/\text{cm}^3$	DL/pptv	$DL^{\text{STP}}/\mu\text{g m}^{-3}$
HCN	3.00	3337.139	2.997	36.89	5.97	179	23.3	6.3	23	0.028
H ₂ CO	2.34	2781.035	3.596	11.86	5.17	155	8.41	17	65	0.087
H ₂ O ₂	2.26	1284.205	7.787	4.464	3.52	105	4.27	34	130	0.2
HNO ₃	2.17	1694.321	5.902	2.85	3.75	112	2.53	58	220	0.60
CH ₃ Cl	1.89	3040.220	3.289	0.192	4.12	123	0.174	840	3100	7.1
HF	1.82	7855.643	1.273	7.591	2.09	362	2.73	54	200	0.18
HCOOH	1.70	1113.068	8.984	4.4	3.32	99	4.4	34	130	0.26
SO ₂	1.59	1371.695	7.290	4.855	3.86	116	4.11	36	130	0.38
NH ₃	1.47	930.757	10.744	52	2.92	88	61.8	2.4	9	0.007
HCl	1.18	2944.914	3.396	50.33	4.30	129	45.1	3.2	12	0.02
H ₂ S	1.02	1364.601	7.328	0.102	4.89	147	0.0685	2100	8000	12
OCS	0.79	2052.716	4.872	103	3.55	106	100	1.5	5	0.015
HBr	0.79	2649.092	3.775	4.456	2.90	87	5.69	26	96	0.35
O ₃	0.53	1052.848	9.498	4.2	2.64	79	5.30	28	100	0.22
HJ	0.38	2277.519	4.391	0.208	2.21	66	0.338	430	1600	9.2
NO ₂	0.29	1600.413	6.248	21.8	2.78	83	27.7	5.3	20	0.042
N ₂ O	0.17	2236.224	4.472	100.4	3.55	106	103	1.4	5	0.01
NO	0.16	1875.813	5.331	3.399	3.26	98	3.91	38	140	0.19
CO	0.10	2169.198	4.610	46.15	3.63	109	48.9	3	11	0.014
C ₂ H ₂	-	3260.427	3.067	22.9	5.43	163	16.5	8.9	33	0.038
CO ₂	-	2270.290	4.405	3.358	3.51	105	3.50	42	160	0.31
CH ₄	-	3067.300	3.260	21.29	5.77	173	15.3	9.6	36	0.026

centrations of trace gases and intercomparisons of TDLAS instruments and conventional systems have been performed to assure data quality [51]. Data from such an intercomparison of NO₂ measurement techniques between an OPSIS DOAS-instrument, a chemiluminescence instrument, and a FM-TDLAS system show that when the air is well mixed due to wind speed above 2 m s⁻¹ there is a good agreement between the longpath measurement of DOAS and the point measurement of TDLAS, whereas the chemiluminescence instrument shows differences, although measuring at the same point as the TDLAS [52]. The International Organization for Standardization (ISO) has specified in its regulation "Air quality — determination of performance characteristics of measurement methods" (ISO/DIS 9169) procedures to quantify calibration function and its linearity, the lower detection limit and precision of the instrument. To measure these characteristics, calibration gases with mixing ratios in the expected concentration range have to be used. The generation of calibration gases in the low ppbv and sub-ppbv range, however, is a difficult task. Therefore, part of our work has been focused on the development of a calibration device in compliance with the ISO requirements for an integrated tunable diode laser spectrometer, which is based on permeation devices with a subsequent flow dilution [51]. The system can be used as a secondary standard and allows multi-component as well as multi-point calibrations of TDLAS and similar instruments. The performance of the FM-TDLAS instrument has been characterized by a calibration function and the method was found to be linear within the tested range.

Among volatile organic compounds (VOC's), oxygenated compounds such as aldehydes and ketones are of particular importance as one of the major sources of free radicals in the atmosphere. Continuous measurements of formaldehyde can presently be carried out using methods based on enzymatic reactions and fluorometric detection and the direct spectroscopic measurement by tunable diode laser absorption spectroscopy. The TDLAS technique is almost free of interferences and, therefore, can be used as a reference method for the validation of less specific techniques in the

frame of quality assessment studies [53]. As the primary oxidizing agent responsible for the removal of most trace gases, the hydroxyl radical, OH, is central to the chemistry of the troposphere [16]. OH is closely linked to the HO₂ radical through reactions with NO, CO, O₃ and hydrocarbons. HO₂ is present, typically, at concentrations of about 10⁸ mole cm⁻³, which is about 100 times that of OH, and has a chemical lifetime of a few minutes. Currently different approaches to measure HO₂ are partly realized or under discussion [53]. One of them is tunable diode laser absorption spectroscopy, which is very specific but has not yet been demonstrated in the laboratory. We have investigated in detail the feasibility of HO₂ measurements by the FM-TDLAS technique. The measurement of HO₂ radicals is still a great challenge, but the future measurement by the FM-TDLAS technique seems to be feasible [53].

The importance of hydrogen peroxide, H₂O₂, in atmospheric chemistry [54] arises from its oxidizing potential in the liquid phase and from the fact of being involved in gas- and liquid-phase radical chemistry. Formaldehyde is another important photoactive trace component of the atmosphere. Measurements in clean air provide an important insight into the removal processes of light hydrocarbons as well as information about the general chemical reactivity of the atmosphere [55]. Only a few measurements of the formaldehyde concentrations in the remote marine troposphere have been made, but different background levels were reported. Therefore, continuous measurements of hydrogen peroxide and formaldehyde have been carried out onboard the German research vessel *Polarstern*, where for the first time with a two-component high-frequency modulated TDL system has been used for the detection of trace gases over the Atlantic Ocean on a route from the northern to the southern hemisphere (50° N – 50° S).

Another important measurement challenge is the direct determination of trace gas fluxes by the eddy correlation technique through a plane parallel to the surface [16]. For the determination of surface emission and deposition fluxes, the method is rigorous when specific criteria are met. The technique requires simultaneous fast and ac-

curate measurements of both the vertical velocity and the trace species in question. Fortunately the technique for the measurement of the turbulence with the necessary resolution is available. Sonic anemometers can readily yield air motion data with the required resolution. Likewise, the ability to handle the air motion and chemical concentration data with modern computer systems is well in hand. Thus these aspects can be ignored, and the major limitation can be dealt with: the availability of appropriate chemical sensors with sufficient time and chemical resolution. The FM-technique is ideally suited for flux measurements by the eddy correlation method [56,57] and future developments should increase the number of trace gases, which can be investigated.

7. Summary and conclusions

The routine measurement of a great number of trace gases poses challenging requirements to analytical techniques. Thus, sensitive, selective and portable instruments, which are even capable of multicomponent analysis are required. Apart from flexibility as the molecule of interest is concerned, the ease of operation as well as the usefulness for field applications also have to be considered for practical evaluations. Although the current instrumentation is sufficient for many applications, still better detection limits are required by modern atmospheric research. Substantial improvements of TDLAS detection speed and detection limits were obtained by introducing high frequency modulation techniques. However, to achieve this sensitivity improvement and to build instruments for routine high sensitivity measurements, many practical problems still have to be solved. It was the purpose of this paper to illustrate the current state-of-the-art in FM spectroscopy and to discuss new approaches to solve some of the problems that currently limit system performance. For optimum performance, FM-TDLAS instruments need high quality diode-lasers and have to be designed to ensure long term stability, which is needed for ultrasensitive measurements. For mid-IR applications the lasers presently available have to be improved substan-

tially towards higher power and single mode emission in order to avoid laser excess noise. The transmission of multi-pass absorption cells has to be increased and turbulence effects have to be reduced in order to obtain a quantum limited performance. With increasing detection limits, the improved performance can be utilized to obtain more precise measurements, even at higher concentrations. This is especially important for the future under aspects of quality control and quality assurance.

Acknowledgements

This work was funded by the German Ministerium für Forschung und Technologie (BMFT) under grant 08431095, 07EU702 and 07EU712 as a contribution to the EUROTRAC subproject JETDLAG and by the Bayerisches Staatsministerium für Wirtschaft und Verkehr (3625-VIII/4c).

References

- [1] H.I. Schiff, G.I. Mackay and J. Bechara, in M.W. Sigrist (Ed.), *Air Monitoring by Spectroscopic Techniques*, Wiley, New York, 1994.
- [2] D.J. Brassington, in R.E. Hester and R.J. Clark (Eds.), *Advances in Spectroscopy Vol. 24: Spectroscopy in Environmental Science*, Wiley, New York, 1994.
- [3] R. Grisar, H. Böttner, M. Tacke and G. Restelli (Eds.), *Monitoring of Gaseous Pollutants by Tunable Diode Lasers*, Kluwer, Dordrecht, 1992.
- [4] A.I. Nadezdinskii and A.M. Prokhorov (Eds.), *Tunable Diode Laser Applications*, Proc. SPIE, 1724 (1992).
- [5] H.I. Schiff and U. Platt (Eds.), *Optical Methods in Atmospheric Chemistry*, Proc. SPIE, 1715 (1993).
- [6] J. Reid, J. Shewchun, B.S. Garside and A.E. Ballik, *Appl. Opt.*, 17 (1978) 300.
- [7] R.S. Inman and J.J.F. McAndrew, *Anal. Chem.*, 66 (1994) 2471.
- [8] R. Kästle, R. Grisar, M. Tacke, D. Dornisch and C. Scholz, *Microcontamination*, 11 (1991) 27.
- [9] E.V. Stephanov and K.L. Moskalenko, *Opt. Eng.*, 32 (1993) 361.
- [10] D.E. Cooper, R.U. Martinelli, C.B. Carlisle, H. Riris, D.B. Bour and R.J. Menna, *Appl. Opt.*, 32 (1993) 6727.
- [11] M. Haverlag, E. Stoffels, W. Stoffels, H. den Boer, G. Kroesen and F. de Hoog, *Jpn. J. Appl. Phys.*, 33 (1994) 4202.

- [12] J. Lawrenz and K. Niemax, *Spectrochim. Acta*, 44B, (1989) 155.
- [13] J.C. Camparo, *Contemp. Phys.*, 26 (1985) 443.
- [14] C.E. Wieman and L. Hollberg, *Rev. Sci. Instrum.*, 62 (1991) 1.
- [15] R.M. Measures (Ed.), *Laser Remote Chemical Analysis*, Wiley, New York, 1988.
- [16] L. Newman (Ed.), *Measurement Challenges in Atmospheric Chemistry*, Am. Chem. Soc., Washington, DC, 1993.
- [17] G.C. Bjorklund, *Opt. Lett.*, 5 (1980) 15.
- [18] D.E. Cooper and T.F. Gallagher, *Appl. Opt.*, 24 (1984) 1327.
- [19] M. Gehrtz, W. Lenth, A.T. Young and H.S. Johnston, *Opt. Lett.*, 11 (1986) 132.
- [20] C.B. Carlisle, D.E. Cooper and H. Preier, *Appl. Opt.*, 28 (1989) 2567.
- [21] P. Werle, F. Slemr, M. Gehrtz and Chr. Bräuchle, *Appl. Phys. B*, 49 (1989) 99.
- [22] D.S. Bomse, A.C. Stanton and J.A. Silver, *Appl. Opt.*, 31 (1992) 718.
- [23] J.M. Supplee, E.A. Whittaker and W. Lenth, *Appl. Opt.*, 33 (1994) 6294.
- [24] P. Werle, *J. Phys. Fr.* IV, 4 (1994) 9.
- [25] P. Werle, R. Mücke and F. Slemr, *Appl. Phys. B*, 57 (1993) 131.
- [26] P. Werle, *Appl. Phys. B*, 60 (1995) 499.
- [27] R.S. Eng, A.W. Mantz and T.R. Rodd, *Appl. Opt.*, 18 (1979) 1088.
- [28] P. Werle, F. Slemr, M. Gehrtz and Chr. Bräuchle, *Appl. Opt.*, 28 (1989) 1638.
- [29] H. Fischer and M. Tacke, *J. Opt. Soc. Am. B*, 8 (1991) 1824.
- [30] R. Großkloß, P. Kersten and W. Demtröder, *Appl. Phys. B*, 58 (1994) 137.
- [31] P. Werle and F. Slemr, *Appl. Opt.*, 30 (1991) 430.
- [32] M. Osinsky and J. Buus, *IEEE J. Quant. Electron.*, 23 (1987) 9.
- [33] W. Lenth, *IEEE J. Quant. Electron.*, 20 (1984) 1045.
- [34] C.R. Webster, *J. Opt. Soc. Am. B*, 2 (1985) 1464.
- [35] D.W. Allan, *Proc. IEEE*, 54 (1966) 221.
- [36] W. Demtröder, *Laser Spectroscopy*, Springer, Berlin, 1982, p. 225.
- [37] R. Schieder, G. Rau and B. Vowinkel, *Proc. SPIE*, 598 (1985) 189.
- [38] A. Fried, H. Riris and G. Harris, personal communication, 1994.
- [39] H. Riris, C.B. Carlisle, L.W. Carr, D.E. Cooper, R.U. Martinelli and R.J. Menna, *Appl. Opt.*, 33 (1994) 7059.
- [40] J.U. White, *J. Opt. Soc. Am.*, 66 (1976) 411.
- [41] D.R. Herriott and H.J. Schulte, *Appl. Opt.*, 4 (1964) 883.
- [42] J.B. McManus, P.L. Kebabian and M.S. Zahniser, *Appl. Opt.*, 34 (1995) 3336.
- [43] P. Werle, *Infrared Phys. Technol.*, 37/01 (1996) 59–66.
- [44] P. Werle and B. Jänker, *Opt. Eng.*, 35 (7) (1996).
- [45] H.-J. Clar, R. Schieder, M. Reich and G. Winnewisser, *Appl. Opt.*, 28 (1989) 1648.
- [46] J.S. Barlent jr. and A.W. Mantz, *Appl. Opt.*, 31 (1992) 1907.
- [47] H. Riris, C.B. Carlisle, R.E. Warren and D.E. Cooper, *Opt. Lett.*, 19 (1994) 144.
- [48] P. Werle, B. Scheumann and J. Schandl, *Opt. Eng.*, 33 (1994) 3093.
- [49] E.A. Whittaker, H.R. Wendt, H.E. Hunziker and G.C. Bjorklund, *Appl. Phys. B*, 35 (1984) 105.
- [50] P. Werle and B. Jänker, *Technisches Messen*, 3 (1996) 92.
- [51] R. Mücke, B. Scheumann, F. Slemr and P. Werle, *Proc. SPIE*, 2112 (1994) 87.
- [52] L. Martini, R. Sladkovic, F. Slemr and P. Werle, *Proc. of the 87th Annual Meeting of the Air & Waste Management Association*, Cincinnati, OH, 1994.
- [53] R. Mücke, F. Slemr and P. Werler, *The Proceedings of EUROTRAC Symposium '94*, P.M. Borrell et al. (Eds.), SPB Academic Publishig BV, The Hague, The Netherlands, 1994, p. 915.
- [54] F. Slemr, G.W. Harris, D.R. Hastie, G.I. Mackay and H.I. Schiff, *J. Geophys. Res.*, 91 (1986) 5371.
- [55] G.W. Harris, G.I. Mackay, T. Iguchi, L.K. Mayne and H.I. Schiff, *J. Atmos. Chem.*, 8 (1989) 119.
- [56] M.S. Zahniser, D.D. Nelson, J.B. McManus and P.L. Kebabian, *Phil. Trans. R. Soc. Lond. A*, 351 (1995) 371.
- [57] F.G. Wienhold, H. Frahm and G.W. Harris, *J. Geophys. Res.*, 99 (1994) 16567.